FULL PAPER

Cationic Polyfluorenes with Phosphorescent Iridium(III) Complexes for Time-Resolved Luminescent Biosensing and Fluorescence Lifetime Imaging

Huifang Shi, Huibin Sun, Huiran Yang, Shujuan Liu, Gareth Jenkins, Wei Feng, Fuyou Li, Qiang Zhao, Bin Liu,* and Wei Huang**

The application of a time-resolved photoluminescence technique and fluorescence lifetime imaging microscopy for biosensing and bioimaging based on phosphorescent conjugated polyelectrolytes (PCPEs) containing Ir(III) complexes and polyfluorene units is reported. The specially designed PCPEs form 50 nm nanoparticles with blue fluorescence in aqueous solutions. Electrostatic interaction between the nanoparticles and heparin improves the energy transfer between the polyfluorene units to Ir(III) complex, which lights up the red signal for naked-eye sensing. Good selectivity has been demonstrated for heparin sensing in aqueous solution and serum with quantification ranges of 0–70 μM and 0–5 μM, respectively. The signal-to-noise ratio can be further improved through time-resolved emission spectra, especially when the detection is conducted in complicated environment, e.g., in the presence of fluorescent dyes. In addition to heparin sensing, the PCPEs have also been used for specific labeling of live KB cell membrane with high contrast using both confocal fluorescent cellular imaging and fluorescence lifetime imaging microscopies. This study provides a new perspective for designing promising CPEs for biosensing and bioimaging applications.

1. Introduction

Conjugated polyelectrolytes (CPEs) have gained increasing attention in sensor and bioimaging applications over the years.[1] CPEs exhibit several unique advantages such as highly π-electron delocalized backbone structures and fast intra- and inter-chain energy transfer, which result in amplified signal output and increased sensitivity as compared to that based on counterpart small molecules.[2] In addition, CPEs are soluble in polar solvents, such as water, which makes them suitable for in vitro and in vivo sensing and imaging applications.[3] The sensing and imaging performances of CPEs, however, often suffer interference from background, such as the biosubstrate autofluorecence. Moreover, the contamination of fluorescent dyes in the analyte solution can directly complicate the sensing and imaging results. Although small-molecule probes with excitation and emission wavelengths in the near-infrared (NIR) range have been developed to minimize the background interference,[4] NIR CPEs are difficult to obtain because of their complicated molecular design and synthesis.

Phosphorescent heavy-metal complexes (PHMCs) with long emission lifetimes offer an effective means of eliminating undesirable background fluorescence by time-resolved photoluminescence technique (TRPT).[5] The background interference with a short emission lifetime can be eliminated by exerting a time delay between photoexcitation and signal acquisition to yield a high signal-to-noise (S/N) ratio. In addition, the long emission lifetimes allow the isolation of phosphorescence signals from other factors that contribute to the total photoluminescence and selection of long-lived phosphorescence images by fluorescence lifetime imaging microscopy (FLIM).[5,6] Aside from the long emission lifetimes, PHMCs exhibit other merits, such as large Stokes shifts and high

H. Shi, H. Sun, H. Yang, Prof. S. Liu, Prof. G. Jenkins, Prof. Q. Zhao, Prof. W. Huang
Key Laboratory for Organic Electronics & Information Displays (KLOEID)
Jiangsu-Singapore Joint Research Center for Organic/Bio Electronics & Information Displays, and Institute of Advanced Materials (IAM)
Nanjing University of Posts and Telecommunications
Wenyuan Road 9, Nanjing City,
Jiangsu Province, 210046, China
E-mail: iamqzhao@njupt.edu.cn; wei-huang@njupt.edu.cn

H. Shi, Prof. B. Liu
Department of Chemical and Biomolecular Engineering
4 Engineering Drive 4
National University of Singapore
(NUS) 117576, Singapore
E-mail: cheliub@nus.edu.sg

Dr. W. Feng, Prof. F. Li
Department of Chemistry
Fudan University
Shanghai, 200433, China

DOI: 10.1002/adfm.201202385

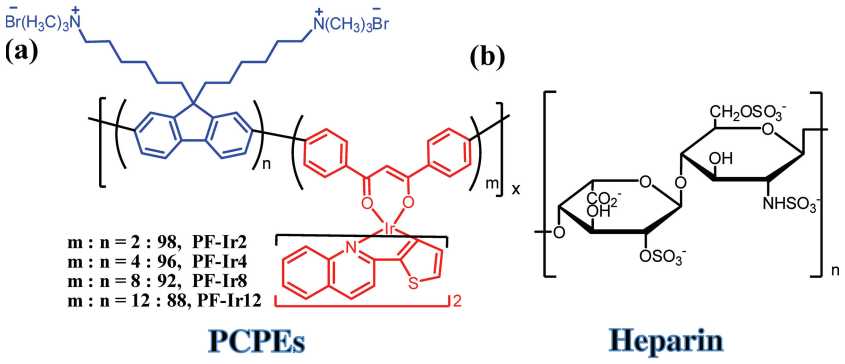

Scheme 1. Chemical structures of the a) synthetic PCPEs and b) heparin.

photostability.[7] Considering the amplified signal output for CPEs and the long emission lifetime for PHMCs, it is ideal to introduce PHMCs (as energy guest) into fluorescent CPEs (as energy host) to yield phosphorescent conjugated polyelectrolytes (PCPEs), which could serve as very promising bioprobes for time-resolved luminescent sensing and fluorescence lifetime imaging applications.

Several requirements for the design and development of PCPEs-based bioprobes are discussed as follows. Firstly, good water solubility is preferred as most biological media are aqueous systems. Secondly, PHMCs with an emission lifetime longer than several hundreds of nanoseconds should be selected to eliminate the background fluorescence via TRPT and FLIM techniques. Thirdly, the content of PHMCs in PCPEs should be optimized to ensure distinguishable emission color or emission change in the presence and absence of analytes; Fourthly, effective spectral overlap between the fluorescent host and the phosphorescent guest is required to achieve efficient energy transfer. Lastly, high luminescence quantum yield and photostability are also very important to allow low power excitation and to minimize photobleaching.

Here, we report the synthesis of water-soluble PCPEs and demonstrate their applications in time-resolved luminescent heparin sensing and fluorescence lifetime imaging of KB cell membrane. The PCPEs are cationic polyfluorenes containing different contents of phosphorescent Ir(III) complexes in their backbones (**Scheme 1**a). Heparin was chosen as the analyte (Scheme 1b), because it is widely used as an injectable anticoagulant in clinical applications to prevent the clots formation in the blood and heparin overdose can cause severe complications during heparin therapy.[8] Traditional methods including activated clotting time (ACT) or activated partial thromboplastin time (aPTT) for heparin detection are indirect, inaccurate and time consuming.[9] Although several fluorescent probes based on small-molecule fluorophores,[10] CPEs,[11] and nanomaterials,[12] have also been developed for heparin sensing, few of them can be applied to real blood samples.[12b] The synthesized PCPE probes compare favorably over the existing probes in heparin sensing in water, serum and patient blood samples. In addition, the triplet emitter enables time-resolved luminescence sensing with eliminated background fluorescence and enhanced signal-to-noise ratio. As recent studies show that CPEs are promising fluorescence imaging materials,[13] the application of the developed PCPEs on KB cell membrane staining is further demonstrated using both confocal fluorescence and fluorescence lifetime imaging microscopies, even in the presence of short-lived background fluorescence.

2. Results and Discussion

2.1. Synthesis and Characterization

Four PCPEs were synthesized in 75–85% yields with different contents of phosphorescent Ir(III) complex. The feed ratios of Ir(III) complex to the total monomers were 2, 4, 8, and 12 mol%; and the corresponding polymers were named as PF-Ir2, PF-Ir4, PF-Ir8 and PF-Ir12, respectively. The polymer structures were characterized by ^{1}H NMR, ^{13}C NMR and elemental analysis. The weight-average molecular weights of the PCPEs range from 6,400 to 27,000 with polydispersity indexes in the range of 1.42–2.28 as determined by GPC (Table S1 in the Supporting Information, SI). The Ir(III) complex contents in the polymers are estimated to be 1.7–10.1 mol% via ^{1}H NMR. It is reasonable that the actual Ir(III) complex contents in the polymers are lower than the feed ratios due to the different reactive activities and/or the steric hindrance effect of the Ir(III) complex segments.[14] Transmission electron microscopy (TEM) and laser light scattering (LLS) were used to study the morphologies of PCPEs in water. As shown in Figure S1 in the Supporting Information, nanoparticles (NPs) with sizes of approximately 45–70 nm are formed in aqueous solutions for all the four PCPEs. In addition, the zeta-potential of PF-Ir4 was measured to be 32.98 mV, which allows the NPs to interact with anionic heparin through electrostatic interactions.

2.2. Photophysical Properties

The absorption and emission spectra of PCPEs in aqueous solutions are shown in Figure S2 (Supporting Information). The polymer concentrations are calculated using polymer repeat units (RU) based on the feed ratios. The main absorption bands at 380 nm for PF-Ir4 and PF-Ir8 and at 360 nm for PF-Ir2 and PF-Ir12 are attributed to the absorption of π–π* transitions of the polymer backbones. The difference is largely caused by the different polymerization degree (Figure S2, Table S1 and S2, Supporting Information). In addition, a weak absorption band at 400–550 nm assigned to the metal-to-ligand charge-transfer (MLCT) transition of the Ir(III) complex is observed, which becomes more evident with the increase of Ir(III)-complex content in the polymers.[15] In PL spectra, a major emission band at 420 nm and shoulders at 440 and 465 nm assigned to the polyfluorene units, as well as a red emission band at 632 nm attributed to Ir(III) complex were observed for all the polymers. The intensity of the red emission gradually increases with the increase of the Ir(III)-complex content in the polymers due to a more efficient energy transfer from the host to the guest. In addition, the emission spectra for PCPEs in films were also

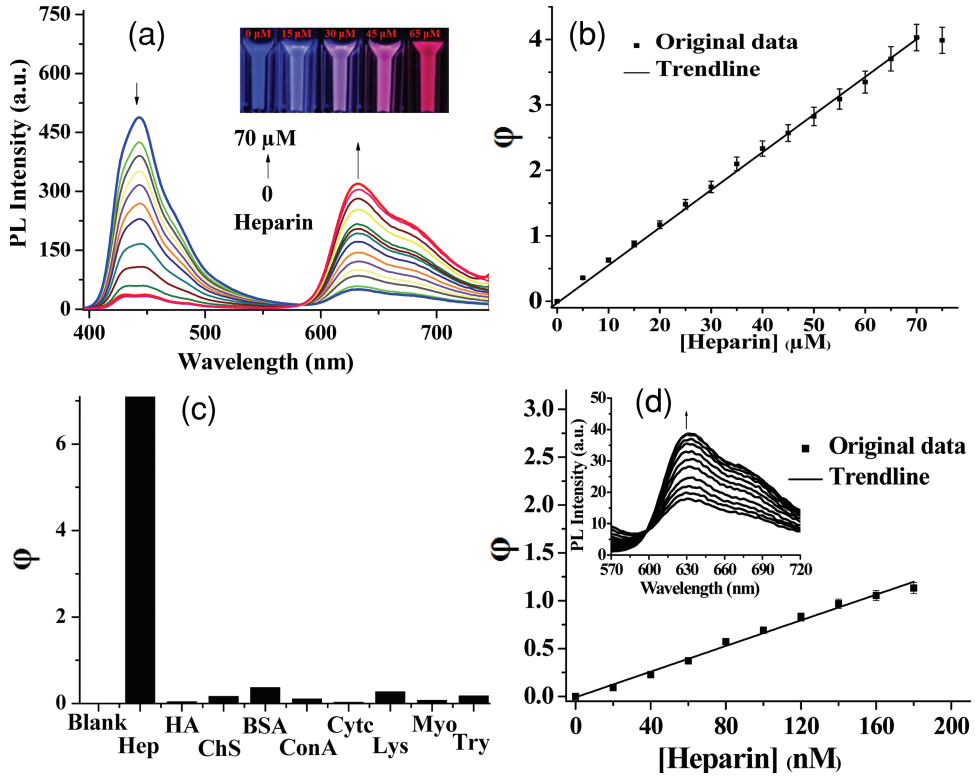

Figure 1. a) PL spectra of PF-Ir4 in HEPES buffer with addition of heparin from 0 to 70 μM upon excitation at 380 nm. Inset: emission color changes of solution under hand-held UV-lamp excited at 365 nm. b) ϕ as a function of heparin concentration and its trendline at [RU] = 135 μM. c) ϕ as a function of PF-Ir4 in the presence of heparin and its analogues, HA and ChS, as well as some biomacromolecules. d) ϕ as a function of heparin concentration and its trendline at [RU] = 5 μM. Inset: the corresponding PL spectra of PF-Ir4 with addition of heparin. The data in panels (b,d) were obtained based on the average of three independent experiments. Hep, HA, ChS, BSA, ConA, Cyct, Lys, Myo and Try stand for heparin, hyaluronic acid, chondroitin sulfate, bovine serum albumin, concanavalin A, cytochromec, lysozyme, myoglobin and trypsin, respectively.

investigated and the results are shown in Figure S3 (Supporting Information). The films were prepared by spin-coating the stock solutions of polymers in methanol. Even for PF-Ir2 with the lowest Ir(III)-complex content, its PL spectrum in film exhibits the obvious red emission at 630 nm assigned to Ir(III) complex. For the films of PF-Ir8 and PF-Ir12, strong red emissions from Ir(III) complex are observed in the PL spectra, while there is almost no blue emission from the fluorene units. These results indicate that the energy transfer is more efficient in films as compared to that in solution for the PCPEs due to the compact polymer aggregates in films, which favor more efficient energy transfer from the polyfluorene host to the Ir(III) guest.

2.3. Heparin Detection

As mentioned earlier, the content of Ir(III) complex in polymer should be optimized to achieve a significant spectral change upon analyte binding. PCPEs with high Ir(III) complex content, such as PF-Ir8 and PF-Ir12, show obvious background red emission in aqueous solution before analyte addition (Figure S4, Supporting Information),[16] which is undesirable in designing probes with large ratiometric spectral changes.[11a] The use of PF-Ir2 with low Ir(III) complex content is also not ideal due to the low red emission both before and after analyte addition (Figure S5, Supporting Information). As such, PF-Ir4 was chosen for heparin sensing because of its low background red signal and a relatively high Ir(III)-complex content.

Heparin titration experiments were carried out for PF-Ir4 at [RU] = 135 μM in 5 mM HEPES buffer solution (pH 7.4 at 25 °C). The changes in PL spectra of PF-Ir4 upon addition of heparin ranging from 0 to 70 μM at intervals of 5 μM are shown in **Figure 1**a. The PL spectrum of free PF-Ir4 solution is dominated by the blue fluorescence at 443 nm from polyfluorene, and the red phosphorescent emission at 632 nm from Ir(III) complex is weak. Upon addition of heparin, the red emission intensity at 632 nm enhances gradually at the expense of the blue emission at 443 nm with a clear isosbestic point at 584 nm, realizing the ratiometric detection. The ratios of emission intensities at 632 and 443 nm ($I_{632\ nm}/I_{443\ nm}$) exhibit a dramatic change from 0.1:1 to 9.0:1. Such a large change (90-fold) of emission intensity ratios at two wavelengths indicates that PF-Ir4 is an excellent ratiometric fluorescent probe. Furthermore, the difference between two emission wavelengths is large (189 nm) and there is almost no overlap between the two emission bands, which leads to accurate measurement of two emission intensities to yield the ratiometric value. In addition, the large ratiometric value also allows clear visualization of the

solution fluorescent color change. In the absence of heparin, the solution fluorescent color is dark blue, which turns to light blue when [heparin] = 15 μM (inset in Figure 1a). With the further increase in heparin concentrations, the emission color turns to royal purple, followed by pink, and finally red at [heparin] = 65 μM. The red emission band reaches its maximum at 70 μM heparin and remains stable even with further addition of heparin. The distinguishable emission color change at different heparin concentrations enables naked-eye quantification of heparin.

To quantify the heparin concentration in solution, changes of red emission intensity at 632 nm in the presence of various concentrations of heparin are shown in Figure 1b. To simplify the process, a parameter ϕ was defined as follows:

$$\varphi = (I - I_0)/I_0$$

where I_0 is the PL intensity of PF-Ir4 at 632 nm in the absence of heparin and I is the PL intensity with different heparin concentrations. ϕ as a function of heparin concentration together with its linear trendline are shown in Figure 1b, from which a good linear relationship in the heparin concentration from 0 to 70 μM is demonstrated. As the heparin concentration at the therapeutic dosing level is 0.2–8.0 U/mL (1.8–72.0 μM),[11] the results indicate that the PCPE-based heparin probe is promising in clinical applications.

The analogues of heparin, hyaluronic acid (HA) and chondroitin sulfate (ChS), were chosen to investigate the selectivity of PF-Ir4 for heparin. Their chemical structures are shown in Scheme S1 (Supporting Information). The experiments were conducted at [RU] = 135 μM in 5 mM HEPES buffer at pH 7.4. Heparin (65 μM), HA (65 μM) and ChS (65 μM) were added into three blank polymer solutions. A 193-fold increase in PL intensity at 632 nm for heparin over HA and 45-fold over ChS are obtained (Figure 1c), which suggest good selectivity of the PF-Ir4 probe for heparin sensing. Moreover, addition of the same amount of heparin into PF-Ir4/HA and PF-Ir4/ChS mixtures can still induce the red phosphorescence, which shows good competitive ability for heparin (Figure S7,S8, Supporting Information). Aside from HA and ChS, other six biomacromolecules including bovine serum albumin, concanavalin A, cytochromec, lysozyme, myoglobin and trypsin, were also used to study the selectivity of PF-Ir4. As shown in Figure 1c and Figure S9 (Supporting Information), no significant change in the PL spectra (especially the red emission region) was observed upon addition of these biomacromolecules, which indicates good selectivity of the probe for heparin sensing.

Another titration experiment was conducted in a diluted PF-Ir4 solution with [RU] = 5 μM in 5 mM HEPES buffer at pH 7.4 to determine sensitivity of the heparin assay. The changes in PL spectra upon addition of various amounts of heparin ranging from 0 to 180 nM at intervals of 20 nM are shown in the inset of Figure 1d. An obvious increase in the red emission intensity of PF-Ir4 solution is observed upon addition of 20 nM heparin, which indicates that the detection limit is lower than 20 nM. ϕ as a function of heparin concentration and its trendline are shown in Figure 1d. A good linearity shows that the PCPE assay for heparin quantification can be realized in the range of 0–180 nM under the experimental condition.

To demonstrate the potential application of PF-Ir4 in biological media, further study was conducted for heparin detection at [RU] = 60 μM in 5 mM HEPES buffer with 5% fatal bovine serum (FBS). As shown in **Figure 2**a, the PL intensity for PF-Ir4 at 632 nm increases upon addition of heparin from 0 to 6 μM, although the background red emission intensity is obvious in the absence of heparin due to the polymer/FBS interaction. A notable emission color change from blue to pink makes the naked-eye detection for heparin possible in serum (inset in Figure 2a).

As heparin is widely used as an injectable anticoagulant in clinical applications, we also attempted to detect heparin in real patient blood samples. In this study, four blood samples from different patients were applied. The experiments were carried out using PF-Ir4 [RU] = 30 μM in 5 mM HEPES buffer containing 1% (volume ratio) patient blood samples. As shown in Figure 2b, a remarkable change in the PL intensity ratio ($I_{632\ nm}/I_{450\ nm}$) is observed after addition of 5 μM heparin to

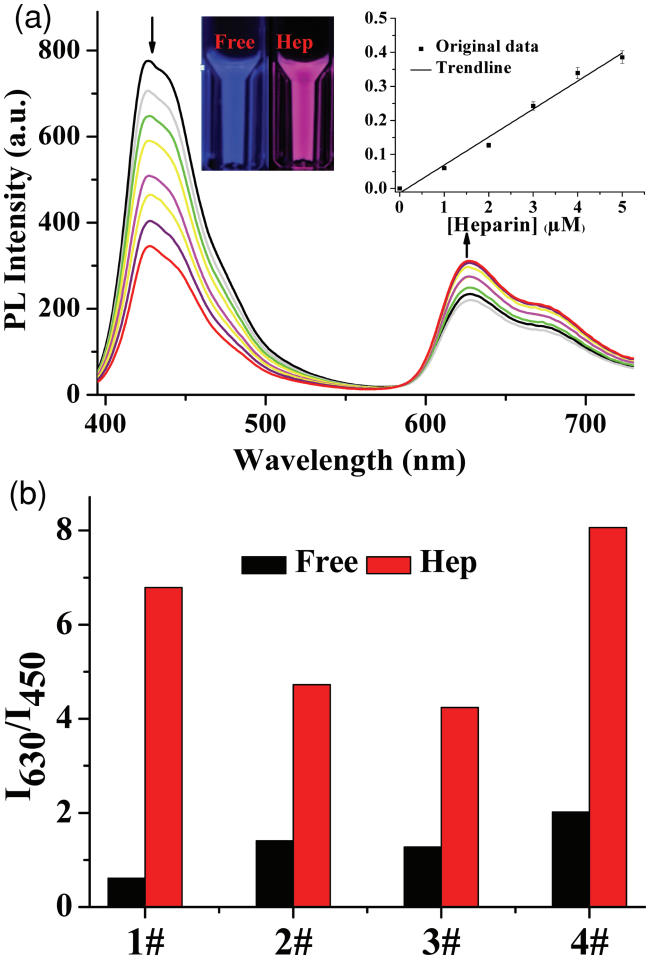

Figure 2. a) PL spectra of PF-Ir4 at [RU] = 60 μM in 5 mM HEPES buffer containing 5% FBS at pH 7.4 upon addition of heparin from 0 to 6 μM. Inset: ϕ as a function of heparin concentration and its trendline and emission color changes of solution under hand-held UV-lamp excited at 365 nm. b) PL intensity ratio ($I_{632\ nm}/I_{450\ nm}$) changes of PF-Ir4 at [RU] = 30 μM in HEPES buffer containing 1% patient blood samples (1#–4#) in the absence (black) and presence (grey) of heparin.

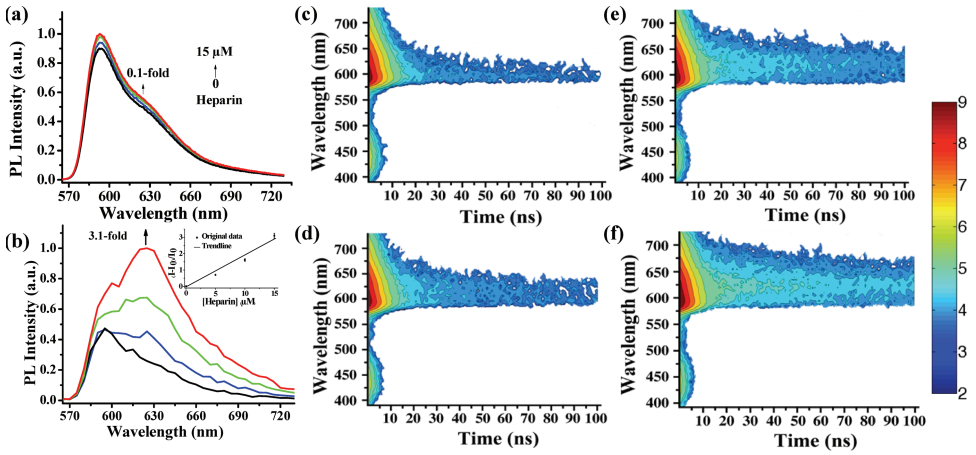

Figure 3. PL spectra of PF-Ir4/RB mixture in 5 mM HEPES buffer with addition of heparin from 0–15 μM a) in a steady state and b) at delayed time of 99 ns. Inset shows the linear tendency. RT TRES (excited at 379 nm) of PF-Ir4/RB at various heparin concentrations: c) 0 μM; d) 5 μM; e) 10 μM; and f) 15 μM.

each blood sample. As far as we know, this is the first report of heparin detection in patient blood samples using CPE-based probes. These results show that PCPE-based probes could be promising tools for heparin detection in real clinical applications through further optimization.

In practical applications, the validity and accuracy of the probes is inevitably interfered with undesirable background fluorescence, which is generally short-lived. The most attractive merit of PCPEs is their long emission lifetime of phosphorescent signal. For PF-Ir4, the emission lifetime of the red phosphorescence at 632 nm is as long as 223 ns in air equilibrated solution, which is suitable for time-resolved luminescent detection. To demonstrate the concept, a fluorescent dye, Rhodamine B (RB) with a short emission lifetime of 2.1 ns, was selected as the signal interference, whose emission can significantly overlap with the red phosphorescence from Ir(III) complex of PF-Ir4 (Figure S10, Supporting Information). The experiments for time-resolved emission spectra (TRES) were carried out at [RU] = 30 μM in 5 mM HEPES buffer solution containing RB (50 μM) upon addition of heparin from 0 to 15 μM at intervals of 5 μM at room temperature. The steady-state PL spectra were recorded as shown in **Figure 3**a. The maximum emission at 590 nm was assigned to RB and a shoulder at 632 nm was attributed to Ir(III) complex from PF-Ir4. Almost no change in the PL spectra is observed upon heparin addition, which indicates the strong interference of background fluorescence to heparin sensing. However, distinct emission changes in TRES after a delay of 99 ns were observed with a 3.1-fold increase in the phosphorescent emission intensity (Figure 3b). The inset in Figure 3b shows the linear tendency with various amounts of heparin, which indicates that heparin sensing could be realized in complicated media through time-resolved photoluminescent technique. The TRES of PF-Ir4 with addition of different amounts of heparin are displayed in Figure 3c–f. The phosphorescent emission intensity at 632 nm increases with the increased heparin concentration, whereas the fluorescence from RB is removed after the time delay between photoexcitation and acquisition of signals. This result indicates that the PCPEs are promising bioprobes that can be applied in complicated environment.

2.4. Sensing Mechanism

To understand the excellent sensing performance, the sensing mechanism of PF-Ir4 for heparin was subsequently investigated in details. The self-assembly of PF-Ir4/heparin complexes was examined by laser light scattering (LLS). The NPs of PF-Ir4 were formed at [RU] = 135 μM in 5 mM HEPES buffer solution. The particle size distributions of PF-Ir4 and PF-Ir4/heparin complexes are depicted in **Figure 4**. A unimodal distribution peak is observed for free PF-Ir4 solution, indicating the formation of NPs with a mean diameter of 51 nm. The NP size increases with the addition of heparin. When [heparin] is 35 μM, the mean diameter of NPs becomes 75 nm. Further increase the heparin concentration to 65 μM leads to complexes with a mean diameter of 92 nm. At this point, the solution becomes charge balanced between the oppositely charged polymer and heparin. An excess amount of heparin ([heparin] = 90 μM) further enlarges the NP size to 109 nm.

The morphologies of PF-Ir4 in the absence and presence of heparin were further investigated through TEM. The polymer itself forms NPs with an average diameter of 40–60 nm (**Figure 5**a). A core-shell structure was formed for PF-Ir4/heparin complex (Figure 5b). The core size is approximately 20–40 nm and the whole NP size is larger than 60 nm. We tentatively propose that polymer cores were enveloped by heparin as the shell through electrostatic interaction to form the core-shell structures. The nanoscale binding between PF-Ir4 and heparin can induce the polymer NPs to be more compact (Figure 5b,c), which favors both intra- and inter-chain energy transfer from polyfluorene to Ir(III) complex, leading to the observed ratiometric signal change. To further test this hypothesis, the zeta potential for PF-Ir4/heparin complex at the charge-balance state was also measured to be–23.96 mV. The negative charge on the PF-Ir4/heparin complex surface further supports the proposed mechanism.

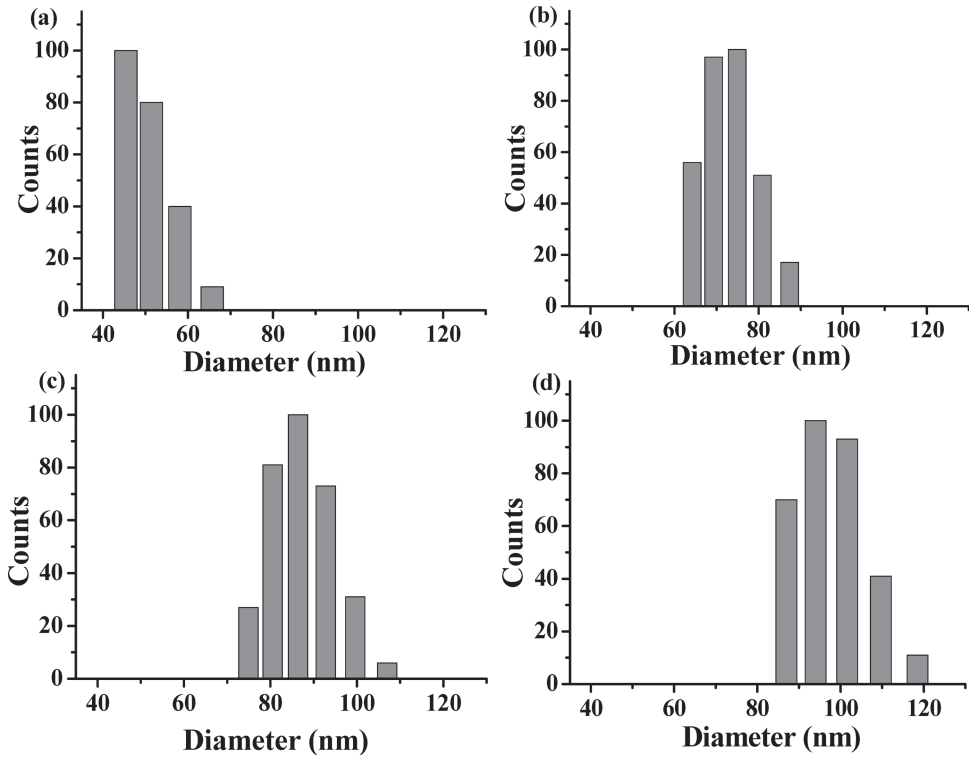

Figure 4. LLS of PF-Ir4 at [RU] = 135 μM in 5 mM HEPES buffer solution at different concentrations of heparin. a) [heparin] = 0 μM; b) 35 μM; c) 65 μM; and d) 90 μM.

2.5. Cellular Imaging

To demonstrate the potential of PCPEs in cellular imaging, the confocal images of living KB cells after incubation with PF-Ir4 in PBS buffer at pH 7 are shown in **Figure 6**. The emission collected at 430–460 nm (Figure 6b) is assigned to the polyfluorene segment and the emission collected at 600–650 nm is due to phosphorescent Ir(III) complex (Figure 6c). From the overlay image (Figure 6d), both the blue and red luminescences emerge from the cell surface, indicating that the polymer can be used to stain the cell membrane. This is confirmed by Z-scan image of the PF-Ir4 stained cells (Figure S12, Supporting Information) and the same cells co-stained with 1,1′-dioctadecyl-3,3,3′,3′-tetramethylindocarbocyanine perchlorate (DiI). The bright field, luminescence and overlay images are shown in **Figure 7**. The green (Figure 7a) and red (Figure 7b) emissions are from the membrane dye DiI and Ir(III) complex of the polymer, respectively. The good overlap between the locations of the signal from the polymer and DiI further verifies that PCPEs can specifically stain the cell membrane.

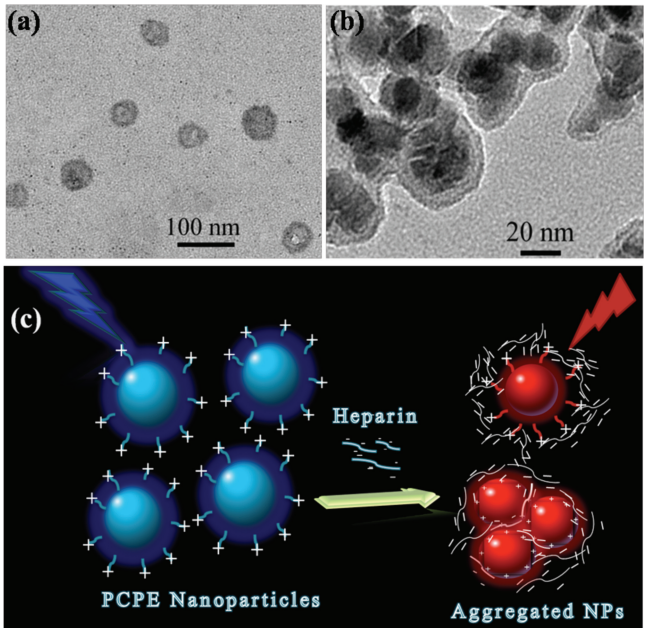

Figure 5. TEM images of PF-Ir4 in the a) absence and b) presence of heparin in aqueous solution. c) Illustration of the possible sensing mechanism.

To demonstrate the merits of long phosphorescence lifetime in bioimaging, FLIM was performed on fixed Hela cells after incubation with both PF-Ir4 (40 μg/mL) and fluorescein isothiocyanate (FITC) (20 μM) in PBS buffer at pH = 7. The luminescent images of Hela cell are shown in **Figure 8**. The green emission at 520–550 nm (Figure 8a) is mainly assigned to the background short-lived fluorescence from FITC, whereas the red emission at 600–650 nm (Figure 8b) is due to the long-lived phosphorescence from PCPEs. The FLIM results shown in Figure 8c,d and Figure S13 (Supporting Information) indicate that the emission signals from PCPEs on the cell membrane could be distinguished from the interference signal of FITC due to their significant differences in emission lifetimes. This

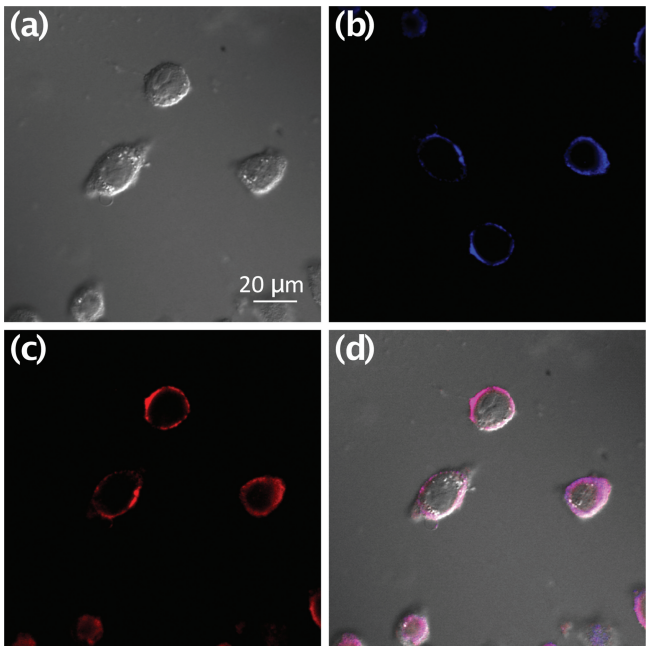

Figure 6. Confocal images of KB cells collected at a) 430–460 nm and b) 600–650 nm, and c) overlay of living KB cells incubated with 40 μg/mL PF-Ir4 in PBS (pH = 7) for 60 min at 37 °C. Excitation wavelength is 405 nm. All the images share the same bar of 20 μm.

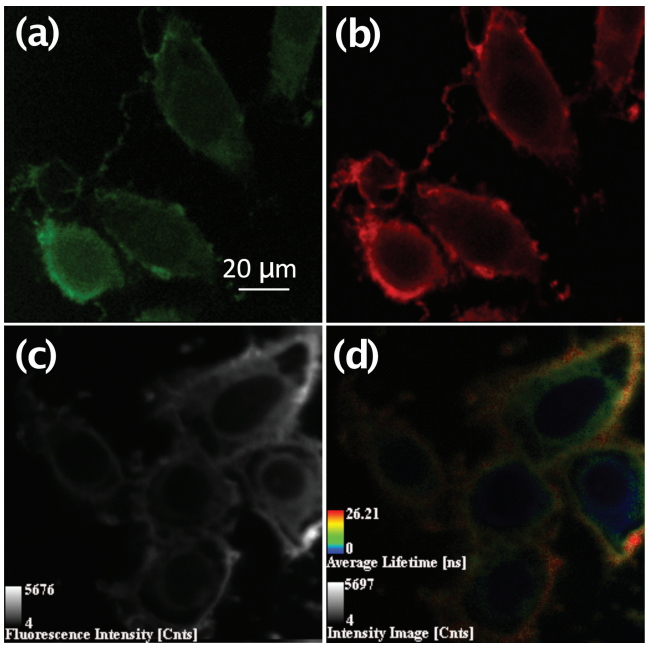

Figure 8. Confocal images of fixed Hela cells incubated with PF-Ir4 (40 μg/mL) and FITC (20 μM) in PBS buffer at pH = 7. Luminescence collected at a) 520–550 nm and b) 600–650 nm. c) Fluorescence intensity image and d) lifetime image upon excitation at 488 nm. All the images share the same bar of 20 μm.

result further demonstrates that the PCPEs are beneficial for selection of long-lived phosphorescence images in the presence of background fluorescence via the FLIM technique.

3. Conclusions

In summary, four PCPEs with different contents of Ir(III) complex have been designed and synthesized, which combine the advantages of both conjugated polyelectrolytes and phosphorescent heavy-metal complexes. A phosphorescent light-up probe for visual heparin sensing with low detection limit and high selectivity has been demonstrated. The probe has allowed heparin quantification in the range of 0–70 μM and 0–5 μM in water and serum, respectively. Furthermore, heparin detection in complicated environment and in real patient blood samples clearly indicates the potential clinical application of the probe, especially with the TRPT technique. In addition to sensing, the developed PCPEs are also promising bioimaging agents for specific staining of the cell membranes. FLIM was applied successfully for selection of long-lived phosphorescence images of cell membranes in the presence of short-lived background fluorescence. To the best of our knowledge, this is the first time CPEs have been used in time-resolved luminescent biodetection and fluorescence lifetime imaging. We believe that the introduction of TRPT and FLIM techniques into CPE-based biosensing and bioimaging will promote more significant development of PCPE-based bioprobes for practical applications.

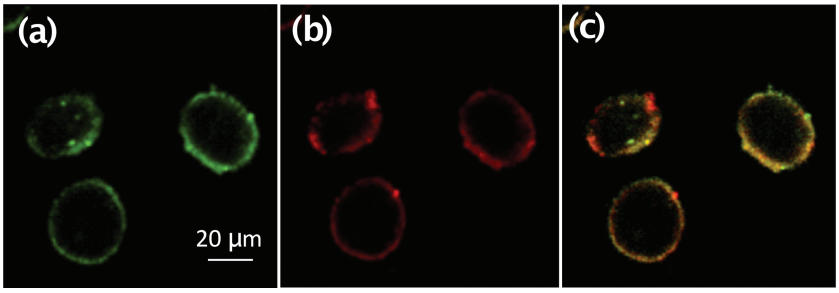

Figure 7. Confocal images of KB cells co-stained with PF-Ir4 and DiI. Luminescence collected at a) 520–560 nm for DiI and b) 600–650 nm for PF-Ir4 upon excitation at 488 nm. The overlay image is shown in (c). [PF-Ir4] = 40 μg/mL and [DiI] = 5 μM in PBS buffer at pH = 7. All the images share the same bar of 20 μm.

4. Experimental Section

Materials and Methods: All chemical reagents, unless otherwise specified, were purchased from Sigma Aldrich Chemical Company. All solvents for reaction and photophysical investigation were of HPLC grade. Fetal Bovine Serum (FBS) was purchased from HyClone. $IrCl_3 \bullet 3H_2O$ was an industrial product and used without further purification. Stock solutions for heparin (2 mM), HA (2 mM) and ChS (2 mM) were prepared in MilliQ water. Heparin molecular weight is calculated by the common repeat unit, which are 644.2 g/mol. Here the heparin has 170 U/mg and 1 μM is equal to 0.11 U/mg. The polymer concentrations were determined by the molecular

weight of the polymer repeat unit (RU), which was calculated through the feed ratios of the polymers. Take PF-Ir4 as an example: its molecular weight is 617.6 g/mol, including 0.04 mol Ir(III)-complex and 0.96 mol (trimethylammonium)hexyl-substituted fluorene. Stock solutions for polymers (1 mM) were prepared in methanol and diluted to different concentrations in 5 mM HEPES buffer aqueous solution. Rhodamine B (10 mM) was prepared in anhydrous ethyl alcohol. Fluorescein isothiocyanate (FITC) (20 μM) and the membrane dye (1,1′-dioctadecyl-3,3,3′,3′-tetramethylindocarbocyanine perchlorate, DiI (5 μM) were prepared in phosphate buffered saline (PBS) buffer at pH = 7. Patient blood samples were obtained from Nanjing First Hospital.

Photoluminescence (PL) spectra were measured on a Perkin Elmer LS-55 with Xe lamp excitation source and a Hamamtsu (Japan) 928 PMT, using a 90 degree angle for solution samples. UV-vis absorption spectra were recorded on a UV-1700 Shimadzu UV-vis spectrophotometer. Nuclear magnetic resonance (NMR) spectra were recorded on Bruker ACF400 (400 MHz) instrument. Mass spectra were obtained on a Bruker autoflex matrix-assisted laser desorption ionization time-of-flight (MALDI-TOF/TOF) mass spectrometer (MS3) and a Shimadzu GCMS-QP2010. The elemental analyses were performed on the Elementar Vario MICRO elemental analyzer. The gel permeation chromatography (GPC) analysis of the polymers was conducted on a Shimadzu 10 Å with THF as the eluent and poly(styrene) as standard. The data were analyzed by using the software package provided by Shimadzu Instruments. Photographs of the solution samples were taken with a Cannon EOC 400D digital camera under a hand-held UV lamp. Average particle size was measured by laser light scattering (LLS) with particle sizing software (90 plus, Brookhaven Instruments Co. USA) at a fixed angle of 90° at RT. Zeta-potential was measured by Zeta-plus zeta potential analyzer. Transmission electron microscopy (TEM) was conducted on a JEOL JEM-2100 transmission electron microscope at an acceleration voltage of 150 kV. Time-resolved emission spectra (TRES) and emission lifetimes were obtained through a time-correlated single photon counting (TCSPC) technique using an Edinburgh FL 920 instrument with a laser (379 nm) as the excitation source. Time-gated acquisition of photoluminescence spectra was performed by employing the TRES technique. Delayed photoluminescence spectra acquired after a 99 ns did not contain fluorescence originating from rhodamine B. Thus, a photoluminescence spectrum with a 99 ns delay was chosen and compared with the total photoluminescence spectrum.

Cell Culture and Imaging: The human nasopharyngeal epidermal carcinoma cell line (KB cells) and the Henrietta Lacks strain of cancer cell lines (Hela cells) were supplied by the Institute of Biochemistry and Cell Biology, SIBS, CAS (China). The cells were grown in RPMI 1640 (Roswell Park Memorial Institute's Medium) supplemented with 10% FBS at 37 °C and 5% CO_2. Cells (5×10^8/L) were placed on 18 mm glass coverslips and allowed to adhere for 24 h.

The cell imaging experiments were carried out with an Olympus FV1000 laser scanning confocal microscope and a 60 X oilimmersion objective lens. A diode laser served as an excitation source at 405 nm for the living KB cells which were incubated with PF-Ir4 (40 μg/mL) solely for 60 min at 37 °C and emission was collected at 420–460 nm and 600–650 nm; excitation at 488 nm for fixed Hela cells incubated with PF-Ir4 (40 μg/mL) for 60 min at 37 °C and further incubated with FITC (20 μM) for 30 min at 37 °C, emission was collected at 520–550 nm and 600–650 nm; excitation at 488 nm for living KB cells incubated with PF-Ir4 (40 μg/mL) for 60 min at 37 °C and further incubated with DiI (5 μM) for 30 min at 37 °C, emission was collected at 520–560 nm and 600–650 nm, respectively. FLIM experiments were conducted on Nikon Instruments A1 Confocal Laser Microscope Series. Fixed Hela cells attached onto a glass slide were covered with a thin glass cover slip, onto which an excitation beam was focused. A 488 nm picosecond pulsed diode laser with 2.5 MHz repetition rate and 0.17 mW laser power was used for excitation.

Supporting Information

Supporting Information is available from the Wiley Online Library or from the author.

Acknowledgements

The authors thank the National Basic Research Program of China (973 Program, 2009CB930601 and 2012CB933301), National Natural Science Foundation of China (Project No. 61274018, 21174064, 21171098), Ministry of Education of China (No. IRT1148), Key Projects in Jiangsu Province for International Cooperation (BZ2010043), Priority Academic Program Development of Jiangsu Higher Education Institutions, Singapore National Research Foundation (R279-000-323-281) and Temasek Defence Systems Institute (ARF R-279-000-305-592/422/232) for financial support.

Received: August 21, 2012
Revised: October 8, 2012
Published online: February 6, 2013

[1] a) A. Duarte, K. Y. Pu, B. Liu, G. C. Bazan, *Chem. Mater.* **2011**, *23*, 501; b) H. Jiang, P. Taranekar, J. R. Reynolds, K. S. Schanze, *Angew. Chem. Int. Ed.* **2009**, *48*, 4300; c) X. L. Feng, L. B. Liu, S. Wang, D. B. Zhu, *Chem. Soc. Rev.* **2010**, *39*, 2411; d) P. F. Sun, X. M. Lu, Q. L. Fan, Z. Y. Zhang, W. L. Song, B. Li, L. Huang, J. W. Peng, W. Huang, *Macromolecules* **2011**, *44*, 8763; e) X. F Liu,. Q. L. Fan, W. Huang, *Biosens. Bioelectron.* **2011**, *26*, 2154; f) C. J. Qin, W. Y. Wong, L. X. Wang, *Macromolecules* **2011**, *44*, 483; g) K. Haskins-Glusac, M. R. Pinto, C. Y. Tan, K. S. Schanze, *J. Am. Chem. Soc.* **2004**, *126*, 14964; h) C. L. Zhu, L. B. Liu, Q. Yang, F. T. Lv, S. Wang, *Chem. Rev.* **2012**, 4687.

[2] a) M. R. Pinto, K. S. Schanze, *Synthesis* **2002**, *9*, 1293; b) B. Kim, I. H. Jung, M. J. Kang, H. K. Shim, H. Y. Woo, *J. Am. Chem. Soc.* **2012**, *134*, 3133; c) C. A. Traina, R. C. Bakus, G. C. Bazan, *J. Am. Chem. Soc.* **2011**, *133*, 12600.

[3] a) K. Lee, J. Lee, J. E. Jeong, A. Kronk, K. S. J. Elenitoba-Johnson, M. S. Lim, J. Kim, *Adv. Mater.* **2012**, *24*, 2479; b) X. L. Feng, G. M. Yang, L. B. Liu, F. T. Lv, Q. Yang, S. Wang, D. B. Zhu, *Adv. Mater.* **2012**, *24*, 637; c) F. M. Ye, C. F. Wu, Y. H. Jin, Y. H. Chan, X. J. Zhang, D. T. Chiu, *J. Am. Chem. Soc.* **2011**, *133*, 8146; d) C. F. Wu, Y. H. Jin, T. Schneider, D. R. Burnham, P. B. Smith, D. T. Chiu, *Angew. Chem. Int. Ed.* **2010**, *49*, 9436; e) K. Li, B. Liu, *J. Mater. Chem.* **2012**, *22*, 1257; f) D. Ding, K. Li, Z. S. Zhu, K. Y. Pu, Y. Hu, X. Q. Jiang, B. Liu, *Nanoscale* **2011**, *3*, 1997; g) C. F. Wu, S. J. Hansen, Q. O. Hou,. J. B. Yu, M. Zeigler, Y. H. Jin, D. R. Burnham, J. D. McNeill, J. M. Olson, D. T. Chiu, *Angew. Chem. Int. Ed.* **2011**, *50*, 3430.

[4] a) Y. Koide, Y. Urano, K. Hanaoka, T. Terai, T. Nagano, *J. Am. Chem. Soc.* **2011**, *133*, 5680; b) A. Palma, L. A. Alvarez, D. Scholz, D. O. Frimannsson, M. Grossi, S. J. Quinn, D. F. O'Shea, *J. Am. Chem. Soc.* **2011**, *133*, 19618; c) Y. H. Chan, F. M. Ye, M. E. Gallina, X. J. Zhang, Y. H. Jin, I. C. Wu, D. T. Chiu, *J. Am. Chem. Soc.* **2012**, *134*, 7309.

[5] a) Y. You, S. Lee, T. Kim, K. Ohkubo, W. S. Chae, S. Fukuzumi, G. J. Jhon, W. Nam, S. J. Lippard, *J. Am. Chem. Soc.* **2011**, *133*, 18328; b) S. W. Botchway, M. Charnley, J. W. Haycock, A. W. Parker, D. L. Rochester, J. A. Weinstein, J. A. G. Williams, *Proc. Natl. Acad. Sci. USA* **2008**, *105*, 16071; c) Y. You, S. Y. Park, *Adv. Mater.* **2008**, *20*, 3820; d) Q. Zhao, F. Y. Li, C. H. Huang, *Chem. Soc. Rev.* **2010**, *39*, 3007; e) S. J. Liu, H. B. Sun, Y. Ma, S. H. Ye, X. M. Liu, X. H. Zhou, X. Mou, L. H. Wang, Q. Zhao, W. Huang, *J. Mater. Chem.* **2012**, *22*, 22167.

[6] a) M. Y. Berezin, S. Achilefu, *Chem. Rev.* **2010**, *110*, 2641; b) L. A. Peteanu, G. A. Sherwood, J. H. Werner, A. P. Shreve, T. M. Smith, *J. Phys. Chem. C* **2011**, *115*, 15607; c) J. Zhang, Y. Fu, D. Liang, K. Nowaczyk, R. Y. Zhao, J. R. Lakowicz, *Nano. Lett.* **2008**, *8*, 1179.

[7] a) Q. Zhao, C. H. Huang, F. Y. Li, *Chem. Soc. Rev.* **2011**, *40*, 2508; b) Q. Zhao, F. Y. Li, S. J. Liu, M. X. Yu, Z. Q. Liu, T. Yi, C. H. Huang,

Inorg. Chem. **2008**, *47*, 9256; c) W. Lu, W. M. Kwok, C. S. Ma, C. T. Chan, M. X. Zhu, C. M. Che, *J. Am. Chem. Soc.* **2011**, *133*, 14120; d) C. Y. Chung, V. W. W. Yam, *J. Am. Chem. Soc.* **2011**, *133*, 18775; e) J. C. H. Chan, W. H. Lam, H. L. Wong, N. Y. Zhu, W. T. Wong, V. W. W. Yam, *J. Am. Chem. Soc.* **2011**, *133*, 12690; f) C. K. Koo, B. Lam, S. K. Leung, M. H. W. Lam, W. Y. Wong, *J. Am. Chem. Soc.* **2006**, *128*, 16434; g) W. Y. Wong, C. L. Ho, *Coord. Chem. Rev.* **2009**, *253*, 1709; h) C. Ulbricht, B. Beyer, C. Friebe, A. Winter, U. S. Schubert, *Adv. Mater.* **2009**, *21*, 4418; i) K. K. W. Lo, A. W. T. Choi, W. H. T. Law, *Dalton Trans.* **2012**, *41*, 6021; j) M. W. Louie, H. W. Liu, M. H. C. Lam, Y. W. Lam, K. K. W. Lo, *Chem. Eur. J.* **2011**, *17*, 8304; k) W. J. Xu, S. J. Liu, X. Y. Zhao, S. Sun, S. Cheng, T. C. Ma, H. B. Sun, Q. Zhao, W. Huang, *Chem. Eur. J.* **2010**, *16*, 7125.

[8] H. B. Nader, S. F. Chavante, E. A. Santos, F. W. Oliveira, J. F. Paiva, S. M. Jeronimo, G. F. Medeiros, L. R. Abreu, E. L. Leite, J. F. Sousa, R. A. Castro, T. Toma, I. L. Tersariol, M. A. Porcionatto, C. P. Dietrich, *Braz. J. Med. Biol. Res.* **1999**, *32*, 529.

[9] T. J. Cheng, T. M. Lin, T. H. Wu, H. C. Chang, *Anal. Chim. Acta* **2001**, *432*, 101.

[10] a) Z. L. Zhong, E. V. Anslyn, *J. Am. Chem. Soc.* **2002**, *124*, 9014; b) A. T. Wright, Z. L. Zhong, E. V. Anslyn, *Angew. Chem. Int. Ed.* **2005**, *44*, 5679; c) Q. Dai, W. M. Liu, X. Q. Zhuang, J. S. Wu, H. Y. Zhang, P. F. Wang, *Anal. Chem.* **2011**, *83*, 6559; d) W. Sun, H. Bandmann, T. Schrader, *Chem. Eur. J.* **2007**, *13*, 7701; e) M. Wang, D. Q. Zhang, G. X. Zhang, D. B. Zhu, *Chem. Commun.* **2008**, 4469; f) S. L. Wang, Y. T. Chang, *Chem. Commun.* **2008**, 1173; g) M. C. Yeung, V. W. W. Yam, *Chem. Eur. J.* **2011**, *17*, 11987.

[11] a) K. Y. Pu, B. Liu, *Adv. Funct. Mater.* **2009**, *19*, 277; b) R. B. Jagt, R. F. Gomez-Biagi, M. Nitz, *Angew. Chem. Int. Ed.* **2009**, *48*, 1995; c) L. P. Cai, R. Y. Zhan, K. Y. Pu, X. Y. Qi, H. Zhang, W. Huang, B. Liu, *Anal. Chem.* **2011**, *83*, 7849; d) R. Y. Zhan, Z. Fang, B. Liu, *Anal. Chem.* **2010**, *82*, 1326.

[12] a) A. C. Rodrigo, A. Barnard, J. Cooper, D. K. Smith, *Angew. Chem. Int. Ed.* **2011**, *50*, 4675; b) H. Yan, H. F. Wang, *Anal. Chem.* **2011**, *83*, 8589.

[13] a) K. Y. Pu, B. Liu, *Adv. Funct. Mater.* **2011**, *21*, 3408; b) D. Tuncel, H. V. Demir, *Nanoscale* **2010**, *2*, 484.

[14] H. F. Shi, S. J. Liu, H. B. Sun, W. J. Xu, Z. F. An, J. Chen, S. Sun, X. M. Lu, Q Zhao, W. Huang, *Chem. Eur. J.* **2010**, *16*, 12158.

[15] D. Y. Yu, Y. Zhang, B. Liu, *Macromolecules* **2008**, *41*, 4003.

[16] C. Y. Li, M. X. Yu, Y. Sun, Y. Q. Wu, C. H. Huang, F. Y. Li, *J. Am. Chem. Soc.* **2011**, *133*, 11231.